 doi:10.20944/preprints202204.0273.v1

Article

Research on The Controllable Interface Response Enhancement of The Textured Pilot Valve

Jing Xu[1] Guiming zhang[1] Shaochao Fan[1] Jing Ni[1] Jiadi Lian[2]*

1. Department of Mechanical Engineering, Hangzhou Dianzi University, Hangzhou, 310018, China
2. Department of Mechanical Engineering, China Jiliang University, Hangzhou, 310018, China

Abstract: Based on the textured controllable interface effect, the dynamic performances of the textured and ordinary pilot valve are analyzed experimentally, and the influence of the textured controllable interface on the response of pilot valve is studied. Results show that when P_{in} is small, the textured surface shortens the reciprocating time of valve core, increasing the flow rate, and speeds up the piston stroke of oil cylinder. The valve core actions much more stable and sensitivity. Meanwhile, combined with the theoretical calculation, the operation mechanism of texturing the pilot valve is analyzed. It is concluded that the stress of textured valve core sealing surface is greater than that of ordinary one, and the pressure difference gradually decreases with the increase of P_{in}, and the flow difference is basically the same as the force on the sealing surface. This indicates that the textured surface improves lubrication characteristics, reduces the friction between components. The textured valve makes the velocity changes gently, and enhances the responsiveness and stability of the valve. Those related results provide a new idea for enhancing the response design of the pilot valve.

Keywords: pilot valve; texture; response; stress; flow field analysis

1. Introduction

At present, the propulsion power of high-tech ships is basically driven by the steam turbine, and the steam quantity can be adjusted timely and accurately by the steam valve to meet the increasing mobility requirements of speeds change and directions change. The pilot valve is a kind of control valve which depends on the oil pressure and electromagnetic signal to change the displacement of the slide valve so as to control the system [1]. The unsteady operation of the pilot valve is the key to the oil engine failure and the weak link of the main steam regulation system. The oil film of pilot valve has the characteristics of medium pollution and flow instability, which can easily lead to problems such as hydraulic clamping, increased leakage, delay of control signal transmission, etc. [2-4], resulting in the imbalance of actuator and control system, and even vibration, eccentric wear and fracture of the valve core. Therefore, how to optimize the clearance of the pilot valve to realize rapid and continuous transportation, forming a complete liquid film, and reducing the friction resistance of valve core movement, improving the response speed, is a burning question in the transportation control of liquid flow.

It is well known that the valve performance is related to clearance flow and friction characteristics. Many scholars pointed out that low frequency and high amplitude vibration of the valve [5], oil pollution [6] and so on are easy to cause friction between the valve stem and sleeve, resulting in the jam phenomenon. Frosina et al. [7] Found that the hydrodynamic force in the valve would reduce the valve performance during the stem displacement. Sun Ping [8] analyzed the response problems of the pilot valve axial force and closing speed of the turbine governing system. Sweeney [9] proposed the hydraulic clamping was caused by the uneven distribution of the hydraulic pressure, and the groove [10] was machined on the valve core to reduce the volume of the valve [11], which affected the lubrication characteristics, improved the clamping problem, but increased the internal

leakage. Lisowski, Wang Yongjiu et al. [12-13] modified the valve core structure to improve the flow field and flow characteristics, and solved the problems of wear and jam of hydraulic servo motor. Those methods could improve the friction characteristics of the liquid film and enhance the response characteristics of the valve, but it had a great impact on the use of the system due to the change of the existing structure or the increase of internal leakage and other new problems.

It is well known that the reasonable texture design can reduce the friction between gas-liquid and gas-solid surfaces. In some special occasions, texture can reduce the vibration and noise of the workpiece. Etsion[16-17] processed texture inside the friction pair of piston ring to enhance the lubrication characteristics of piston ring and reduce friction resistance, and showed the friction force on the textured surface was far less than that on the smooth surface. Pan et al. [18] Found that the microhole texture and vertical microgroove texture were able to effectively reduce the surface roughness of the workpiece. Xiuqing Hao [19] fabricated the microstructures on the inner surface of the hybrid bearing, and showed the micro-texture with reasonable area ratio could significantly reduce the vibration amplitude under water film lubrication. Gherca [20] proposed the textures on the rotor could improve the hydrodynamic performance of the thrust bearing. Liu Honglong [21] carried out an experimental study on the tribological properties of textured surfaces based on the point contact between ball and disc high pairs, and concluded the micro-texture exhibited better lubrication and friction reduction effects at higher frequencies. Haiwu Yu [22] adopted the successive overrelaxation method to obtain the average dynamic pressure of circular, elliptical and triangular texture pits on the sliding direction of bearings in different directions, and the ellipse perpendicular to the sag direction had the best bearing capacity. Yang LJ et al. [23] put forward femtosecond laser modification of micro-textured surface on bearing steel GCr15 to reduce frictional wear and enhance load capacity. Reddy [24] studied the tribological performance of textured parallel sliding contact under mixed lubrication condition, and the texture shape has a significant effect. Han Zhibin et al. [25] tested and analyzed the influence of structural parameters of pit texture on the lubrication performance of graphite materials, results show that the pit texture had a certain anti-friction effect under the condition of water lubrication. The lubrication of the clearance of the pilot valve directly affects the stability and responsiveness, which means it is the same as other friction pair, is expected to pass the friction pair surface texture change operating characteristics.

In view of this, based on the enhancement control between the morphology of textured and performance of the pilot valve, taking the textured controllable interface effect as the breakthrough point, making a new type of core with surface texture by laser marking machine. The flow rate of valve, the corresponding displacement of hydraulic cylinder piston rod and the outlet pressure are studied experimentally. The influence of textured controllable interface on the response of pilot valve is studied. Then based on the fluid lubrication, the operation mechanism of the textured pilot valve is defined, and the interface friction control is realized. Those related results provide a new idea for enhancing the response design of pilot valve.

2. Experiment details

2.1. Pilot valve core treatment

Studies have shown [26] that the shark skin can reduce the fluid resistance because of the special rhombus texture which makes them swim fast. Therefore, proper rhomboid texture can reduce the fluid resistance, accelerating the fluid movement, and effectively improve the dynamic lubrication characteristics.

Fig. 1 shows the sealing section on the outer surface of the core (valve core shoulder) is textured. The surface of the valve core is divided into 30 areas along the circumference, and each area can be approximately regarded as a plane. The valve core center axis is used as the center of rotation, and the fiber laser marking machine processes the design pattern

Preprints (www.preprints.org) | NOT PEER-REVIEWED | Posted: 28 April 2022 doi:10.20944/preprints202204.0273.v1

along the center line of each area. When one area is processed, the valve core needs to rotate 12° to make the next area, until the texture is fully processed.

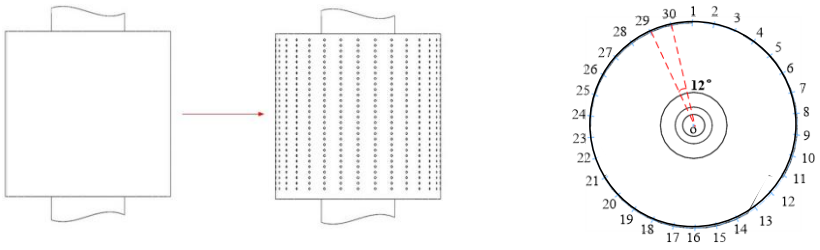

Fig. 1 Preparation of textured valve core diagram

Relevant studies [27] show that the friction coefficient is the minimum when the texture diameter is d=300μm and the depth h=40μm. A rhomboid texture with side length l =300μm, depth h =40μm and angle α=90° between two adjacent sides is designed. The core has five shoulders in direct contact with the sleeve, with a total length of L=90mm. Fig. 2 is the Schematic diagram of textured surface of pilot valve core.

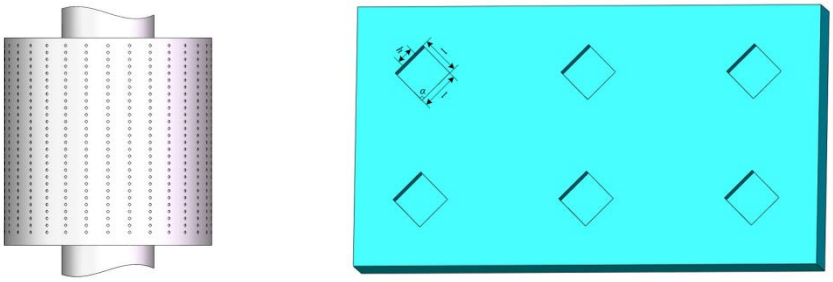

(a) Diagram of shoulder texture surface (b) Schematic diagram of texture model

Fig. 2 Schematic diagram of textured surface of pilot valve core

2.2. Pilot valve experiment design

Fig.3 shows the experimental system diagram of pilot valve. The hydraulic oil enters the pilot valve from port P, and the pilot valve outlet A and B are respectively connected with the cylinder. The secondary oil pressure at port C controls the valve core to move left and right, it makes the pilot valve outlet A and B switch. The port P and C are equipped with a regulating valve to control the pressure at the inlet, and the pressure sensor and flow sensor are installed at the oil inlet of the cylinder to detect the flow and pressure at the inlet of the cylinder. After the secondary oil pressure increasing, the valve core moves right, and the port A channel opens, the power oil enters the cylinder and pushes the piston to move to the left. When the secondary oil pressure drops, the valve core moves left, port B channel opens, the hydraulic oil enters the cylinder and pushes the piston to run to the right. The measured signals of cylinder piston displacement Δx, outlet pressure P and flow Q at port A are detected. The influence of the textured valve core on the performance is studied under different pressure. After smoothing the measured signal curve, Δx, Q, and P dynamic characteristic curves are obtained. The influence of textured valve core on its flow characteristics during the startup process of pilot valve is analyzed.

Preprints (www.preprints.org) | NOT PEER-REVIEWED | Posted: 28 April 2022 doi:10.20944/preprints202204.0273.v1

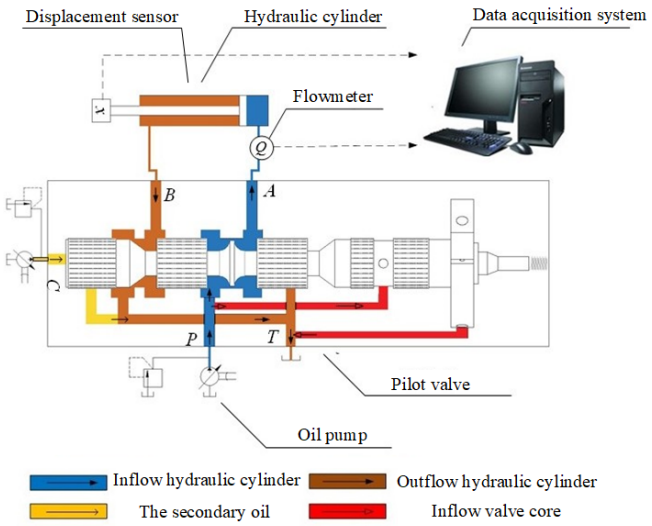

Fig. 3 Experimental system diagram of pilot valve

Fig. 4 shows the corresponding experimental devices such as flowmeter, displacement sensor, pressure sensor and pressure gauge are installed on the experimental system for testing the measured signals such as P, Δx and Q. Table 1 shows the main symbols and meanings in the paper. Table 2 shows the main measuring equipment.

Fig.4 Experimental system of pilot valve

Table 1. Main symbols and meanings in the paper

Symbol	Meaning
P_{in}	Inlet pressure
P	Out pressure
Δx	Cylinder piston displacement
Q	Outlet flow
F	Sealing surface stress

Preprints (www.preprints.org) | NOT PEER-REVIEWED | Posted: 28 April 2022 doi:10.20944/preprints202204.0273.v1

Table 2. Specifications of main experimental instruments

Name	Model	Measurement parameters	Accuracy class
Flowmeter	ECLWGY10ALC2SSN	0.2~1.2m³/h	1%
Displacement sensor	RH-M0500-S1-DN02-A01	0~100mm	0.1%
Pressure sensor	PTh503	0~60MPa	±0.5%
Pressure gauge	YTN-60	0~5MPa	±1.6%

2.3. Results and Discussion

2.3.1. Influence of response on outlet flow

Fig. 5 shows the Q (port A) dynamic characteristic curve of the two kinds of pilot valve. Results show that the flow curve can be divided into three stages. The first stage is the initial stage which only the power oil is fed, and the secondary oil valve port is closed. The second stage is the piston running stage. During this stage, the secondary oil valve port is opened, the valve core moves up, and the Q gradually increases. The third stage is the stable stage which the piston reaches the maximum displacement and Q remains unchanged. When the P_{in} is 0.4MPa to 0.6MPa, the maximum difference between the ordinary and textured pilot valve flow is $\Delta Q_{0.4}$=1m³/h, $\Delta Q_{0.45}$=0.8m³/h, $\Delta Q_{0.5}$=0.5m³/h, $\Delta Q_{0.55}\approx\Delta Q_{0.6}$=0. It can be seen that the Q of the textured pilot valve is always greater than that of the ordinary one, and the textured valve Q reaches the stable stage is much faster than the ordinary one. With the increase of P_{in}, the difference of the Q decreases, and the time difference reaches the stable stage is also narrowing. Q is related to the response speed V of the pilot valve ($Q \propto V$), so the response speed of the textured valve core is higher than that of the ordinary one under low pressure, and the textured surface can improve the response speed of the valve. This indicates the textured surface improves lubrication characteristics, and reduce the friction between components.

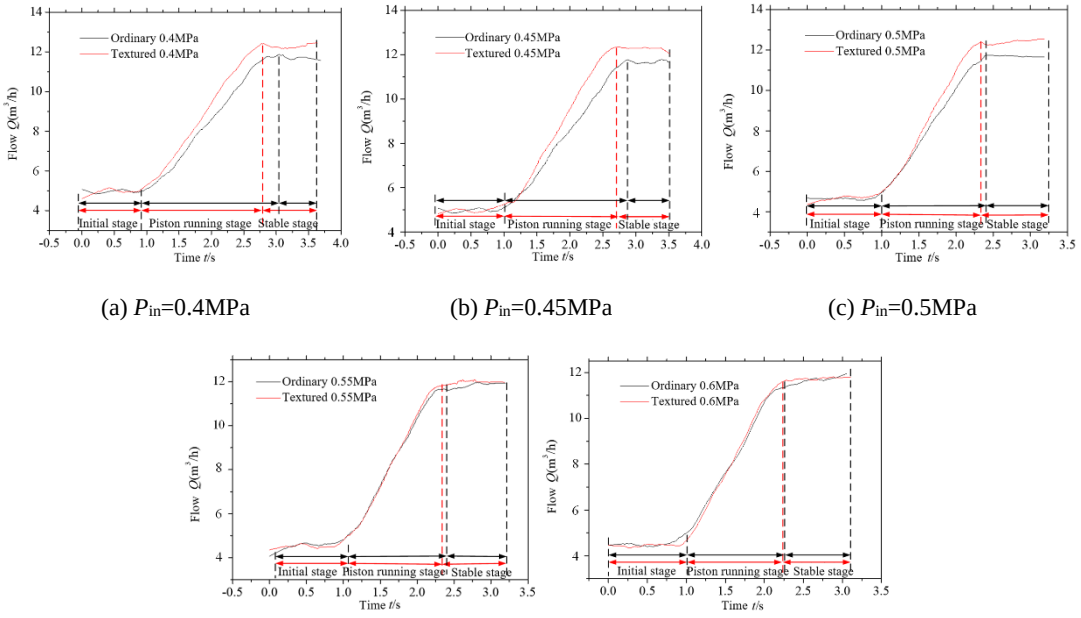

(a) P_{in}=0.4MPa (b) P_{in}=0.45MPa (c) P_{in}=0.5MPa

(d) P_{in}=0.55MPa (e) P_{in}=0.6MPa

Fig. 5 Measured flow curve at port A of pilot valve

Preprints (www.preprints.org) | NOT PEER-REVIEWED | Posted: 28 April 2022 doi:10.20944/preprints202204.0273.v1

2.3.2. Influence of response on piston displacement

Fig. 6 shows the displacement curve of cylinder piston. In the initial stage, the pilot valve at port A is closed, the piston speed V_h=0. In the piston running stage, the pilot valve at port A is opened at point a, the power oil enters the cylinder and pushes the piston out of the cylinder. The piston reaches the maximum displacement at points b and c, and the displacement Δx = 100 mm. In the stable operation stage, Δx reaches the maximum stroke and the operating speed is 0. With the increase of P_{in}, the V_h increases from 3.1cm/s to 8.7cm/s. The V_h of textured pilot valve system is always higher than that of ordinary one. The time difference ΔT between the two pistons to reach the maximum displacement decreases, and the ΔT decreases from $\Delta T_{P=0.4MPa} \approx 0.5$s to $\Delta T_{P=0.6MPa} \approx 0$s. This is because when the P_{in} is low, the textured valve Q is greater than ordinary valve Q, which makes the stroke of the cylinder piston faster. When P_{in}>0.5MPa, Q is almost unchanged, and the V_h is also unchanged. That is consistent with Q analysis results.

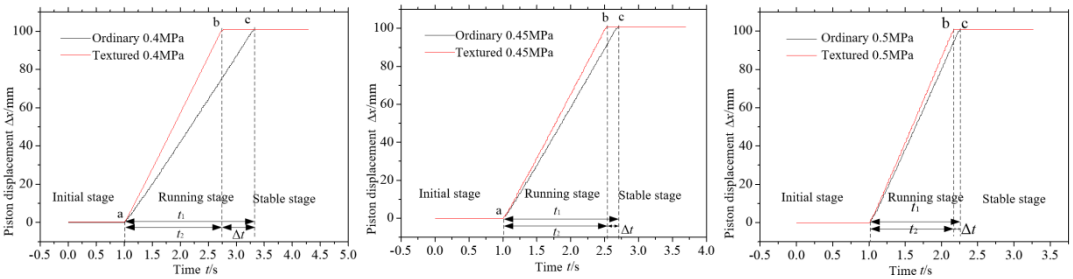

(a) P_{in}=0.4MPa (b) P_{in}=0.45MPa (c) P_{in}=0.5MPa

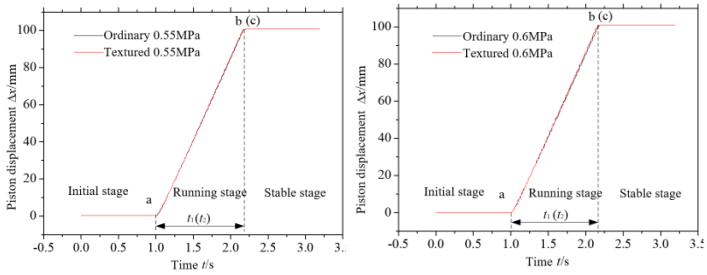

(d) P_{in}=0.55MPa (e) P_{in}=0.6MPa

Fig. 6 Measured displacement curve of cylinder piston

2.3.3. Influence of response on outlet pressure

Fig. 7 shows the dynamic characteristic curve of outlet pressure P. Results show that the P curve also has obvious changes in three stages. During the initial stage ($P \approx 0$) to the piston operation stage, P rises to the first peak and then decreases to a certain value, then remains stable. During the transition from the piston running stage to the stable stage, P rises to another peak in a short time, then decreases to a certain value. The textured valve to reach the peak is faster than that of the ordinary valve. The lower the P_{in}, the faster the textured pilot valve to reach the fixed value. Meanwhile, with the increase of P_{in}, the P difference ΔP_P between the ordinary and textured valve reaching the second peak is smaller, which decreases from $\Delta P_{P=0.4MPa}$= 0.09MPa to $\Delta P_{P=0.6MPa}$=0MPa. The reason is when the piston reaches the maximum displacement, it forms a hydraulic impact, and the reaction force is caused by the hydraulic impact will be fed back to port A. When P_{in}<0.55MPa, the textured valve Q is large and the P is small, the hydraulic impact produced by textured valve is smaller than that of ordinary valve, so the pressure fed back to port A is smaller. When $P_{in} \geq 0.55$MPa, Q and P is close to the same, and the reaction force of hydraulic impact is almost the same. That is consistent with Q and Δx analysis results. Under the condition of low pressure, the textured valve can reduce the hydraulic impact of system in start-stop

Preprints (www.preprints.org) | NOT PEER-REVIEWED | Posted: 28 April 2022 doi:10.20944/preprints202204.0273.v1

condition, it makes the velocity changes gently, and enhances the responsiveness and stability of the valve.

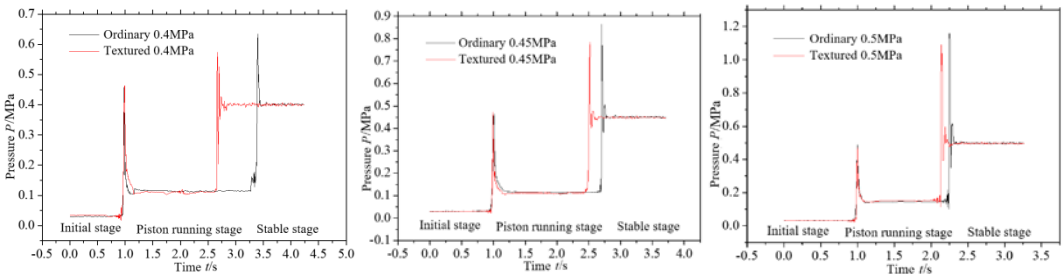

(a) P_{in}=0.4MPa (b) P_{in}=0.45MPa (c) P_{in}=0.5MPa

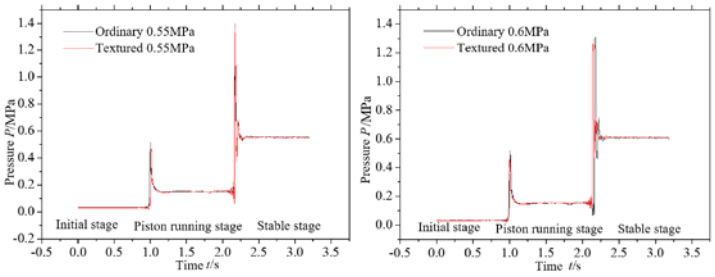

(d) P_{in}=0.55MPa (e) P_{in}=0.6MPa

Fig. 7 Measured outlet pressure curve

3. Research on operation mechanism

Experimental results show that the surface texture can improve the sensitivity of the pilot valve and enhance the response of the controllable interface. Based on the fluid lubrication theory, the internal flow field of valve is numerically calculated, and the operation mechanism of performance is analyzed by studying the stress on the sealing face of valve core and the variation law of outlet flow rate Q.

3.1. Modeling and meshing

The critical Reynolds number of valve clearance fluid flow Re'=2000. The calculation formula of Reynolds number is shown in equation 1.

$$Re = \frac{uD}{\upsilon} \tag{1}$$

Where， u is the average velocity of fluid (m/s), D is the hydraulic diameter (mm), D = 20 mm, and υ is the kinematic viscosity (m^2/s), where, $u=Q/A$, $D=4A/\rho$. According to the above experimental results, Q is the minimum of $0.04m^3/h$, and A is the cross-sectional area of the valve port, so u is calculated to be 127.4m/s. The kinetic viscosity of hydraulic oil υ is $280mm^2/s$, and the Reynolds number Re is 9600, greater than 2000. Therefore, the internal flow field is characterized by turbulence.

The transport equation of turbulent kinetic energy and dissipation rate in k-ε model are

$$\frac{\partial(\rho k)}{\partial t} + \frac{\partial(\rho k u_i)}{\partial x_i} = \frac{\partial}{\partial x_i}\left[\left(\mu + \frac{\mu_i}{\sigma_k}\right)\frac{\partial k}{\partial x_j}\right] + G_k - \rho\varepsilon \tag{2}$$

$$\frac{\partial(\rho\varepsilon)}{\partial t} + \frac{\partial(\rho\varepsilon u_i)}{\partial x_i} = \frac{\partial}{\partial x_j}\left[\left(\mu + \frac{\mu_i}{\sigma_\varepsilon}\right)\frac{\partial \varepsilon}{\partial x_j}\right] + \frac{C_{1\varepsilon}}{k}G_k - C_{2\varepsilon}\rho\frac{\varepsilon^2}{k} \tag{3}$$

Where, $G_k=-\rho\overline{u_i'u_j'}\frac{\partial u_j}{\partial x_j}$ represents the generating term of turbulent kinetic energy, and $k=\frac{1}{2}\overline{u_i'u_j'}$ is the expressions of turbulent kinetic energy k and $\varepsilon=\frac{\mu}{\rho}\left(\frac{\partial u_i'}{\partial x_k}\right)\left(\frac{\partial u_i'}{\partial x_k}\right)$ is the dissipation rate,

$$\mu_i=\rho C_\mu\frac{k^2}{\varepsilon} \tag{4}$$

Here, $C_{1\varepsilon}$=1.44, $C_{2\varepsilon}$=1.92, C_μ=0.09, σ_k=1.0, σ_ε=1.3.

The dynamic characteristics of the pilot valve during normal operation are simulated. The research model is from the pilot valve model 2-8386-2201-07 produced by Hangzhou steam turbine group. Its main structural parameters are as follows: the inlet P diameter 20mm, the outlet A and B diameter 20mm, the valve core stroke 60mm, the valve core diameter 22mm, the valve core shell length 319mm, width and height 120mm.

Due to the complex structure of the pilot valve passage, it is necessary to simplify the inside of the pilot valve passage without affecting the calculation results. The models of the pilot valve fluid domain, ordinary valve core and textured valve core were established, and the mesh was divided. In the process of calculation, the surface of the solid domain needs to be divided into high-quality meshes in order to get more accurate results. Therefore, the pilot valve core was divided into high-quality structured grids. Fig. 8 (a) was the schematic diagram of fluid domain meshing, and Fig. 8 (b) and(c) were the schematic diagram of valve core meshing.

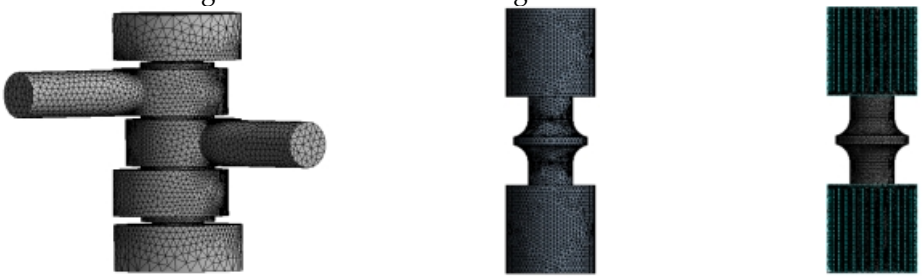

(a) fluid domain meshing (b) ordinary valve core meshing (c)textured valve core meshing

Fig. 8 Meshes of fluid domain and solid domain

To set the boundary conditions, first define the fluid domain type as Fluid Domain, select the calculation time of 500ms and the time step of 0.001s. Secondly, the valve core type was defined as Immersed Solid. The fluid medium was 25°C hydraulic oil, the specific heat capacity was 1800J/(kg·K), the density was 860kg/m^3, the thermal conductivity was 0.12W/(m·K), and the kinematic viscosity was ν=280mm^2/s, dynamic viscosity μ=0.2519Pa·s. The inlet pressure of the pilot valve was 0.4MPa to 0.6MPa, the secondary oil pressure was 0.2MPa, the outlet pressure was 0MPa, and the maximum displacement of the valve core is 20mm.

3.2. Calculation results and discussion

3.2.1. Stress analysis

When the pilot valve is closed, the oil acts on the upper and lower sealing surfaces of the valve core. When the secondary oil pressure changes, the position of the valve core changes accordingly. When the pilot valve is opened, the oil acts on the upper, lower and middle parts of the valve core at the same time. This design controls the change of valve core position through the change of secondary oil pressure, which ensures the operational stability of the pilot valve [28]. The stress on the valve core surface indirectly reflects the contact lubrication state between the valve core and sleeve. The greater the stress, the stronger the bearing capacity of the valve core surface. It can effectively avoid the direct contact between the valve core and sleeve, reducing the friction and wear, and improves the service life and work efficiency. Therefore, four complete stressed sealing

Preprints (www.preprints.org) | NOT PEER-REVIEWED | Posted: 28 April 2022 doi:10.20944/preprints202204.0273.v1

surfaces with or without textured valve core are selected, see Fig. 9, and the stress variation law of the end face of valve core in the opening process of the pilot valve is studied.

(a) (b) (c) (d)

(a)Upper sealing surface of ordinary valve core (c) Upper sealing surface of textured valve core

(b) Lower sealing surface of ordinary valve core (d) Lower sealing surface of textured valve core

Fig. 9 Diagram of sealing surface for different valve core

Fig. 10 shows the stress curves of the upper and lower sealing surfaces of the pilot valve core under different P_{in} during the opening process. Results show that force curves of four sealing surface have the same trendline. The variation of the stress of the upper sealing surface like a parabola, i.e., it climbs up and then declines, while the stress of the lower one varied in another way, i.e., it increases first followed by decreasing, and finally increases again. The stress of the upper sealing surface is always greater than that of the lower one. When P_{in}=0.4MPa, there is a significant stress difference ΔF_s on the upper sealing surface between textured and ordinary surface, and the maximum ΔF_s=79.7N. The lower one ΔF_s between textured and ordinary is more obvious, and the maximum ΔF_x=91.1N. With the increase of P_{in}, ΔF_s gradually weakens, when P_{in}≥0.55MPa, there is no obvious difference, the curves basically coincide. It can be seen that the textured surface can effectively reduce the stress of the friction pairs, and the texture effect gradually decreases with the increase of the P_{in}. This indirectly reflects that the lubrication effect of textured valve is better than that of ordinary one. When P_{in}≥0.55MPa, the texture effect can be ignored. This is consistent with the experimental results.

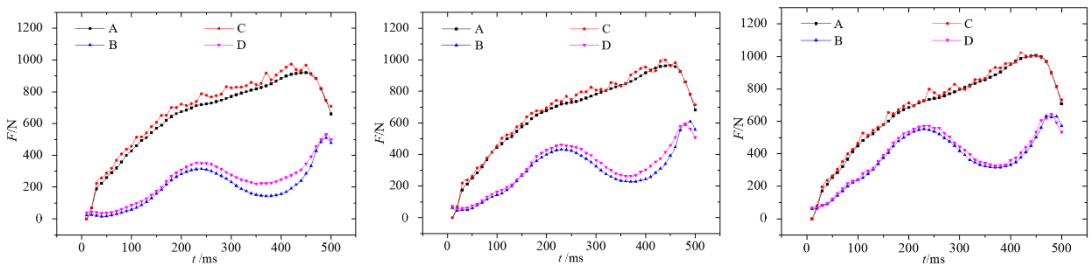

(a) P_{in}=0.4MPa (b) P_{in}=0.45MPa (c) P_{in}=0.5MPa

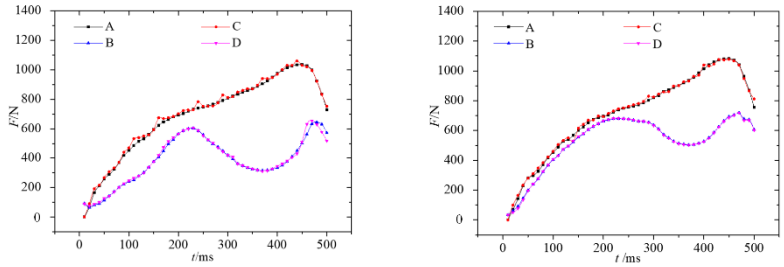

(d) P_{in}=0.55MPa (e) P_{in}=0.6MPa

Fig. 10 Stress change curve of different valve core sealing surface(A is upper sealing surface of ordinary, B is lower sealing surface of ordinary, C is upper sealing surface of textured, D is lower sealing surface of textured)

3.2.2. Flow rate analysis

Fig. 11 shows the variation of outlet flow rate Q with time t during the opening process under different P_{in}. Results show that the Q is changing as the valve core position

Preprints (www.preprints.org) | NOT PEER-REVIEWED | Posted: 28 April 2022 doi:10.20944/preprints202204.0273.v1

change. With the increase of P_{in}, Q between textured and ordinary pilot valve is slightly different. When P_{in}<0.55MPa, the Q of textured valve is obviously larger than that of ordinary valve. The smaller the P_{in} is, the more obvious the Q difference is. When P_{in}≥0.55MPa, the Q of textured valve is almost equal to that of the ordinary valve. This is because the effect of texture on hydrodynamic lubrication increases the sealing clearance and the leakage rate. The lower the P_{in} is, the higher the leakage rate is. When P_{in}≥0.55MPa, the texture effect weakens, the Q difference between textured and ordinary valve can be ignored. That is consistent with stress analysis.

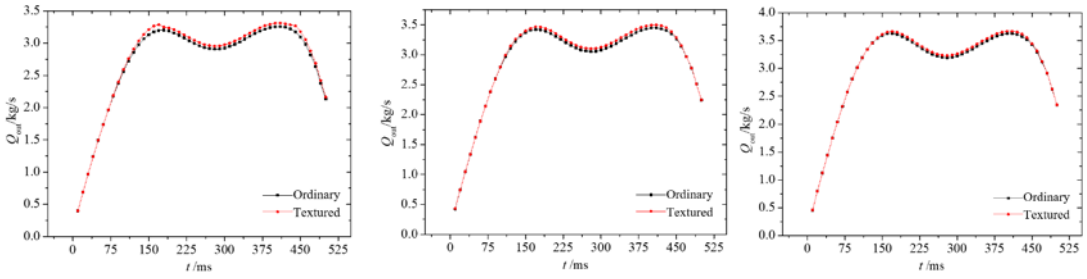

(a) P_{in}=0.4MPa (b) P_{in}=0.45MPa (c) P_{in}=0.5MPa

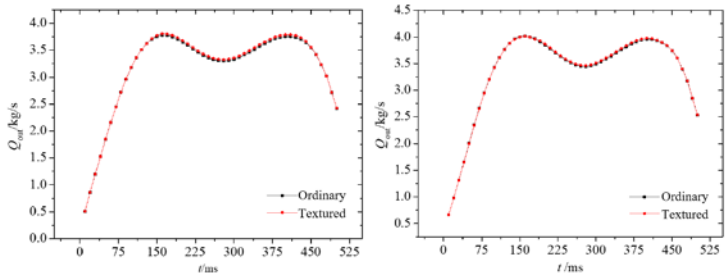

(d) P_{in}=0.55MPa (e) P_{in}=0.6MPa

Fig. 11 Change of outlet flow of different pilot valve

3. Conclusion

Based on the textured controllable interface effect, the dynamic performances of the textured and ordinary pilot valve are analyzed experimentally. Combined with the theoretical calculation, the stress variation law of textured pilot valve during opening process is analyzed.

(1) The flow rate Q, pressure P and displacement of cylinder piston Δx at port A of pilot valve are experimental studied. Results show when P_{in}<0.55MPa, the textured surface shortens the reciprocating time of valve core, increasing the flow rate of port A, and speeds up the piston stroke of oil cylinder, the textured valve actions much more stable and sensitivity. This indicates that the textured surface increases the oil film gap, reduce the friction between components, and effectively improve the dynamic lubrication performance of components. Texture valve core effectively improves the responsiveness of pilot valve. When P_{in}≥0.55MPa, the effect of the textured surface is gradually weakened.

(2) The stress variation law of the upper and lower sealing surfaces of the two kinds of valve cores are computational analysis. Results show when P_{in}<0.55MPa, the stress of textured valve core sealing surface is greater than that of ordinary one, and the stress difference gradually decreases with the increase of inlet pressure P_{in}. The textured surface can effectively reduce the stress of the friction pairs. When P_{in} ≥ 0.55MPa, the stress of textured valve core is basically the same, and the flow difference is basically the same as the force on the sealing surface.

Acknowledgments: The research is financially supported by the Nature Science Foundation of Zhejiang Province, China (No. LY19E050011).

Reference

[1] Shi Yuetao, Ding Xingwu, Gai Yongguang. Steam turbine equipment and operation[M]. China Electric Power Press, 2008: 15-16.

[2] Qi Jinye. Cause analysis and treatment of oil leakage of steam turbine oil seal[J]. Equipment maintenance technology, 2020 (01): 96 + 87.

[3] Wang R . Digital Twin-Driven Mating Performance Analysis for Precision Spool Valve[J]. Machines, 2021, 9.

[4] Zhang Junhui, Lu Zhengyu, Xu Bing, et al. Investigation on the dynamic characteristics and control accuracy of a novel proportional directional valve with independently controlled pilot stage[J]. ISA transactions, 2019, 93.

[5] Liu Z . A Performance Prediction Method for a High-Precision Servo Valve Supported by Digital Twin Assembly-Commissioning[J]. Machines, 2021, 10.

[6] Shuai Fan, Rui Xu, Hong Ji, et al. Experimental Investigation on Contaminated Friction of Hydraulic Spool Valve[J]. Applied Sciences, 2019, 9(23).

[7] Frosina E, Senatore A, Buono D, et al. 3D CFD transient analysis of the forces acting on the spool of a directional valve[J]. Energy Procedia, 2015, 81: 1090-1101.

[8] Sun Ping. Discussion on several problems in dynamic characteristic calculation of steam turbine speed governing system[J]. Thermal power generation, 1993, 1: 29-35.

[9] Sweeny D C. Preliminary investigation of hydraulic lock[J]. Engineering, 1951, 172: 513-6 580-582.

[10] Ye Y, Yin C B, Li X D, et al. Effects of groove shape of notch on the flow characteristics of spool valve[J]. Energy Conversion & Management, 2014, 86(5): 1091-1101.

[11] Zheng Fang, Zhu Dengkui, Lu Chao, et al. Design and experimental research of solenoid directional valve based on 2D Technology[J]. Hydraulics Pneumatics & Seals, 2019(7): 6-8.

[12] Lisowski E, Filo G. CFD analysis of the characteristics of a proportional flow control valve with an innovative opening shape[J]. Energy Conversion & Management, 2016, 123: 15-28.

[13] Wang Yongyong, Lin Sen, Li Yaoqi. Treatment of Cylinder Wall Wear of Steam Turbine Governor Valve Engine[J]. Northeast Electric Power Technology, 2012(5): 32-34.

[14] Nieminen P, Esque S, Muhammad A, et al. Water hydraulic manipulator for fail safe and fault tolerant remote handling operations at ITER[J]. Fusion Engineering and Design, 2009, 84(7-11): 1420-1424.

[15] Watanabe T, Inayama T, Oomichi T. Development of the Small Flow Rate Water Hydraulic Servo Valve[J]. Journal of Robotics and Mechatronics, 2010, 22(3): 333-340.

[16] I. Etsion. Improving tribological performance of mechanical components by laser surface texturing[J]. Tribology Letters, 2004, 17(4): 733-737.

[17] Etsion I. Improving tribological performance of mechanical components by laser surface texturing[J]. Tribology Letters, 2004, 17(4): 733-737.

[18] Pan, Chen, Li, et al. Study on Surface Roughness of Gcr15 Machined by Micro-Texture PCBN Tools[J]. Machines, 2018.

[19] Xiuqing Hao, Helong Sun, Li Wang, et al. Fabrication of micro-texture on cylindrical inner surface and its effect on the stability of hybrid bearing[J]. The International Journal of Advanced Manufacturing Technology, 2020, 109(5-6).

[20] A. Gherca, A. Fatu, M. Hajjam, et al. Influence of surface texturing on the hydrodynamic performance of a thrust bearing operating in steady-state and transient lubrication regime[J]. Tribology International, 2016, 102.

[21] Liu Honglong, Wang Wenzhong, Zhao Ziqiang, et al. Experimental study on effect of surface texture on friction properties of point contact lubrication[J]. Lubrication Engineering, 2014, 39(1): 9-16.

[22] Yu H, Wang X, Zhou F. Geometric shape effects of surface texture on the generation of hydrodynamic pressure between conformal contacting surfaces[J]. Tribology Letters, 2010, 37(2): 123-130.

[23] Lijun Yang, Ye Ding, Bai Cheng, et al. Investigations on femtosecond laser modified micro-textured surface with anti-friction property on bearing steel GCr15[J]. Applied Surface Science, 2018, 434.

[24] Reddy Annadi Ramana, Ismail Syed. Tribological performance of textured parallel sliding contact under mixed lubrication condition by considering mass conservation condition and couple-stress parameter[J]. Proceedings of the Institution of Mechanical Engineers, 2021, 235(2).

[25] Han Zhibin, Wang Lihui, Zhang Xiuli, et al. Effect of pit texture on water lubrication properties of graphite materials[J]. Lubrication Engineering, 2020, 45(12): 81-85+90.

[26] Meng F D, Liu B S, Zeng Y S, et al. Geometric characterization of placoid scales of fast-swimming sharks[J]. Journal of Plasticity Engineering, 2016. 23(2): 143-147.

[27] Tao He, Chuan Li Wang, Hai Shun Deng, et al. Hydrodynamic Lubrication and Load Carrying Capacity Analysis of Laser Surface Texturing Valve Core[J]. Key Engineering Materials, 2016, 4283.

[28] Paolo Tamburrano, Riccardo Amirante, Elia Distaso, et al. Full simulation of a piezoelectric double nozzle flapper pilot valve coupled with a main stage spool valve[J]. Energy Procedia, 2018, 148.